

Scientific paper

Utilization of Corn Cob and TiO₂ Photocatalyst Thin Films for Dyes Removal

Hui-Yee Gan, Li-Eau Leow and Siew-Teng Ong^{1,2,*}

^{1,2} Faculty of Science, Centre for Biodiversity Research, Universiti Tunku Abdul Rahman, Jalan Universiti, Bandar Barat, 31900 Kampar, Perak, Malaysia

> * Corresponding author: E-mail: ongst@utar.edu.my; ongst_utar@yahoo.com Tel: 605-4688888; Fax: 605-4661676

> > Received: 11-10-2016

Abstract

The effectiveness of using TiO₂ and corn cob films to remove Malachite Green oxalate (MG) and Acid Yellow 17 (AY 17) from binary dye solution was studied. The immobilization method in this study can avoid the filtration step which is not suited for practical applications. Batch studies were performed under different experimental conditions and the parameters studied involved initial pH of dye solution, initial dye concentration and contact time and reusability. The equilibrium data of MG and AY 17 conform to Freundlich and Langmuir isotherm model, respectively. The percentage removal of MG remained high after four sorption cycles, however for AY 17, a greater reduction was observed. The removal of both dyes were optimized and modeled via Plackett- Burman design (PB) and Response Surface Methodology (RSM). IR spectrum and surface conditions analyses were carried out using fourier-transform infrared spectrophotometer (FTIR), scanning electron microscope (SEM) and atomic force microscope (AFM), respectively.

Keywords: Malachite Green; Acid Yellow 17; Immoblization; Plackett Burman; Response Surface Methodology

1.Introduction

Dye is a common coloring agent used in textile, paper, ink, food and leather industries. The usage of these dyes has continuously increased and it has been reported that there are more than 100,000 commercial dyes with a rough estimated production of 7×10^5 to 1×10^6 tons per year. Although this colored pollutant imparts only a small fraction of the total organic load in wastewater, it is easily recognizable and damages the aesthetic nature of the environment. Many dyes used in these industries are difficult to degrade, as they are generally stable to light and oxidizing agents, as well as resistant to aerobic digestion. Therefore, conventional effluent treatment methods based on oxidation and/or aerobic digestion may not be effective.

Malachite Green (MG) is a water soluble cationic dye that is widely used in aquaculture as an effective fungicide. However, scientific evidence indicated that MG and its metabolites, leucomalachite green (LMG) is environmentally persistent. This dye causes a serious public health hazards as both clinical and experimental observations reveal that MG is a multi-organ toxin.^{3–5} As MG belongs to the same group of triphenylmethane dyes as cry-

stal violet, in which carcinogenic effects have been demonstrated, therefore based on this group classification, a carcinogenic effect can be assumed.⁴ Acid Yellow 17 (AY 17) is a mono-azo acid dye, widely used in the textile, leather, cosmetic and paper industry. It is also a common additive in household products such as shampoo, detergent, soap and shower gel.⁶ This dye synergizes dermatitis to sensitive skin and causes irritation to eyes. Besides, its thermal decomposition emits toxic fumes of CO, CO₂ and NO.⁷ Due to these severe problems, water contamination originated from the dyeing and finishing in textile industry has become a major concern.

The most common physical method utilized by textile industry for waste water treatment is adsorption. Amongst all, activated carbon is one of the most popular adsorbents and it has also demonstrated its efficiency in the removal of various pollutants. However, this type of adsorbent remains as a costly material and it is difficult to regenerate. Thus, there is a need to continue exploring other economical feasible treatment method for dyes removal. Maize also known as corn, is one of the major feed grains in the world. However, after the removal of corns, the abundant agriculture residues such as corn cob, corn husk,

corn leaf and corn stalk are often burnt without utilization. ^{8,9} But corn cob can actually serves as an attractive low cost adsorbent as it possesses some fairly amazing properties. It contains approximately 39.1% cellulose, 42.1% hemicellulose, 9.1% lignin, 1.7% protein and 1.2% ash. ¹⁰

Apart from adsorption technique, photocatalytic oxidation is also one of the emerging technologies for the elimination of organic pollutants. From the literature, photocatalysis have demonstrated different degrees of applicability for the removal of organic pollutants from aqueous solutions and often, this is viewed as a promising method because it requires no addition of chemicals. 11-15 The basic principle involve can be depicted as follows: once excited by light with energy higher than the band gap energy of photocatalyst, pairs of holes (h⁺) and electrons (e⁻) generate and migrate to the surface to react with adsorbed reactants. The holes, together with other oxidizing species such as hydroxyl radicals resulting from certain photochemical reactions, oxidize the organic pollutants to carbon dioxide, water and some simple mineral acids.16

The main drawback for these two wastewater treatment processes was low economical feasible. Often, extra energy or equipment is required for the post-filtration, centrifugation and sedimentation process. Therefore, in this current work, attempt has been made to immobilize both corn cob and TiO₂ onto a thin film to overcome the problem associated with separation of fine particles mentioned earlier. In order to further enhance the usefulness and efficiency of the proposed treatment method, the percentage uptake for both MG and AY 17 were optimized and modeled via Plackett- Burman design (PB) and Response Surface Methodology (RSM).

2. Materials and Methods

2. 1. Adsorbent

Corn cob was collected from Kampar night market and cut into small pieces, approximately 2 cm/ piece. It was then washed several times with distilled water and consequently boiled for 3 hours to remove the adhering dirt and residues. The clean corn cob was then dried in oven at 60 °C for 24 hours. Dried sorbent was subsequently grinded into powder form and passed through 1 mm sieve before stored into the air tight container for further experimental use.

2. 2. Immobilization of TiO₂ and Corn Cob

Chitosan solution was prepared by dissolving 5.05 g of chitosan powder (coarse ground flakes and powder, Sigma-Aldrich Pte. Ltd) in 500 mL of 1% (v/v) acetic acid solution under continuous stirring for a night at room temperature to ensure all the chitosan powder was well dissolved and the solution was bubble free.

 ${
m TiO_2}$ Degussa P25 (mainly in anatase form, mean particle size of 30 nm, BET surface area of 50 m²/g) was dispersed well and free from agglomeration into chitosan solution via the combination of mechanical stirring and sonication methods with slight modicfication. Both corn cob film (1.0 g of corn cob / 63 g chitosan solution) and ${
m TiO_2}$ film (0.25 g of ${
m TiO_2}$ / 63 g chitosan solution) were prepared with evaporative casting method onto a 10.16×10.16 cm of polymer plate and dried in oven at 45 °C for 24 hours to evaporate all the moisture. The dried films were then neutralized by soaking it in 0.5 M of NaOH solution for 4 hours. Thereafter, the films were washed till neutral pH and subjected for further drying in oven at 35 °C for 24 hours.

2. 3. Adsorbates

Binary dye solution was selected for this study and it involved the mixing of Acid Yellow 17, AY 17 (C.I.= 18965) and Malachite Green crystal, MG (C.I. = 40000). Both dyes were purchased from Sigma-Aldrich Pte. Ltd and were used as received without further purification. The prepared binary dye solution was kept in dark for prevent degradation from light.

2. 4. Instrumental and Characterization Analysis

The functional groups that present on corn cob film before and after dye removal process were determined using Perkin Elmer FTIR, Spectrum RX1 at the wavenumber range of 400–4000 cm⁻¹ with the number of 4 scans *per* sample and resolution of 4.0 cm⁻¹. The surface morphology of corn cob and TiO_2 film was studied by using field emission scanning electron microscope (JEOL FESEM JSM 6701F), operated at emission current of 3.0 kV with working distance of 4.6 mm. Besides, atomic force microscope was also employed (AFM, Park System, XE-70) to observe the surface topography of film before and after the dye removal process by using the contact mode on a $15 \times 15 \ \mu\text{m}^2$ area.

2. 5. Batch Study

Batch study was performed under the exposure of sunlight continuously for 4 hours. Light intensity was recorded at every 1 hour interval with UVA/B light meter. Based on the results from our previous studies in the laboratory, the amount of dyes adsorbed by TiO₂ in dark was negligible. Both TiO₂ thin film and corn cob film were immersed in 500 mL of binary dye solution (10.0 mg/L of MG and 40.0 mg/L of AY 17) in the aquarium tank. Aeration was provided by an air pump. At predetermined time intervals, a known volume of dye solution was withdrawn from the tank and analyzed for its dye content using UV-visible spectrophotometer to determine the % of dye removal. The same experimental conditions were employed

throughout the study unless otherwise stated. The percentage uptake of dye was calculated based on Equation 1.

Percentage removal (%) =
$$\frac{c_o - c_e}{c_o} \times 100 \%$$
 (1)

where,

 C_0 = Initial concentration of dye, mg/L

C_e = Concentration of dye in equilibrium, mg/L

2. 5. 1. Effect of pH

The removal of dyes at different initial pH was investigated in range of pH 4.45 ± 0.50 (natural pH of the binary dye solution) to 7. Dilute sodium hydroxide (NaOH) solution was added dropwise to adjust the pH to the desire pH, prior to the experiment.

2. 5. 2. Effect of Initial Dye Concentrations and Contact Time

The effect of initial dye concentrations and contact time on the percentage uptake of MG and AY 17 was studied by using the dye concentrations of 20, 40 and 80 mg/L. Dye solution was collected at various time intervals, 5, 10, 15, 30, 60, 120, 180, 240 and 300 minutes and the concentration was determined.

2. 5. 3. Sorption Isotherm

Sorption isotherms were obtained by varying the initial dye concentrations of MG from 10.0 mg/L to 50.0 mg/L and 40.0 mg/L to 80.0 mg/L for AY 17. The experiment was carried out by adding 0.1 g of corn cob film into 20 mL of binary dye solutions. This sorption mixture was then shaken at 150 rpm in a centrifuge tube at room temperature for 4 hours.

2. 5. 4. Reusability of TiO₂ Film and Corn Cob Film

The possibility of repetitive usage of films was studied in this parameter. The same TiO₂ and corn cob films were reused for multiple sorption cycles (up to 4 cycles). Before the films were subjected for the next cycle of sorption process, the previously sorbed dyes were removed from the films by soaking it in 0.5 M NaOH solution for desorption process. This was followed by several washings until neutral and the films were air-dry.

2. 6. Statistical Approach

2. 6. 1. Evaluation of Factors Affecting the Percentage Uptake of Dyes

The effect of various factors that influence the percentage uptake of MG and AY 17 were investigated with

Plackett-Burman design. The validity of 3 factors including initial dye concentrations, contact time and initial p-H of binary dye solution were screened by Design Expert Version 7.1.3 software to generate 12 experimental designs.

2. 6. 2. Optimization Study

The factors resulted from Plackett-Burman study was continued with central composite design (CCD) model in Response Surface Methodology (RSM) by using Design Expert Version 7.1.3 software. The correlation of factors and percentage uptake for binary dye was described with modified cubic model.

3. Results and Discussion

3. 1. Instrumental Analysis

3. 1. 1. Fourier Transform Infrared Spectroscopy (FTIR)

Figure 1 shows the FTIR spectra of native chitosan film and corn cob film before and after adsorption in the wavenumber range from 4000 to 400 cm⁻¹. From the spectrum, the peak observed at 3436 and 3437 cm⁻¹ corresponded to the amine stretching N-H and confirmed the presence of amine group in the chitosan structure. The peaks appeared at 2920 cm⁻¹ indicated that the stretching vibration of C-H bond of methylene and methane group, whereas 2844 cm⁻¹ shows C-H stretching for sp³ carbon atom. As for peak observed at 1632, 1638 and 1642 cm⁻¹, this would suggest the presence of N-H bending amine groups. A weak intensity of C=C stretching bands for aromatic rings were assigned at 1425cm⁻¹. It was noticed that the FTIR spectra of corn cob film (before and after adsorption) are very similar to each other. Apart from the limitations in the sensitivity of the instrument, this could also be due to the nature of the process. As it has been postulated that the dye removal process mainly involved adsorption, which is a surface chemistry process, therefore the FTIR spectra before and after the process would shown not much difference. Similar results were reported in the removal of Methylene Blue by using nitrilotriacetic acid modified banana pith.²

3. 1. 2. Surface Characterization

The surface morphology involving shape and porosity of the films was studied using SEM. The SEM micrographs that showed the surface texture of ${\rm TiO_2}$ film and corn cob film before and after the dyes removal process was presented in Figures 2 and 4. The analysis was performed under the magnification of $10,000 \times$.

From these SEM micrographs, it is apparent that before the dyes removal process, TiO₂ powders has been

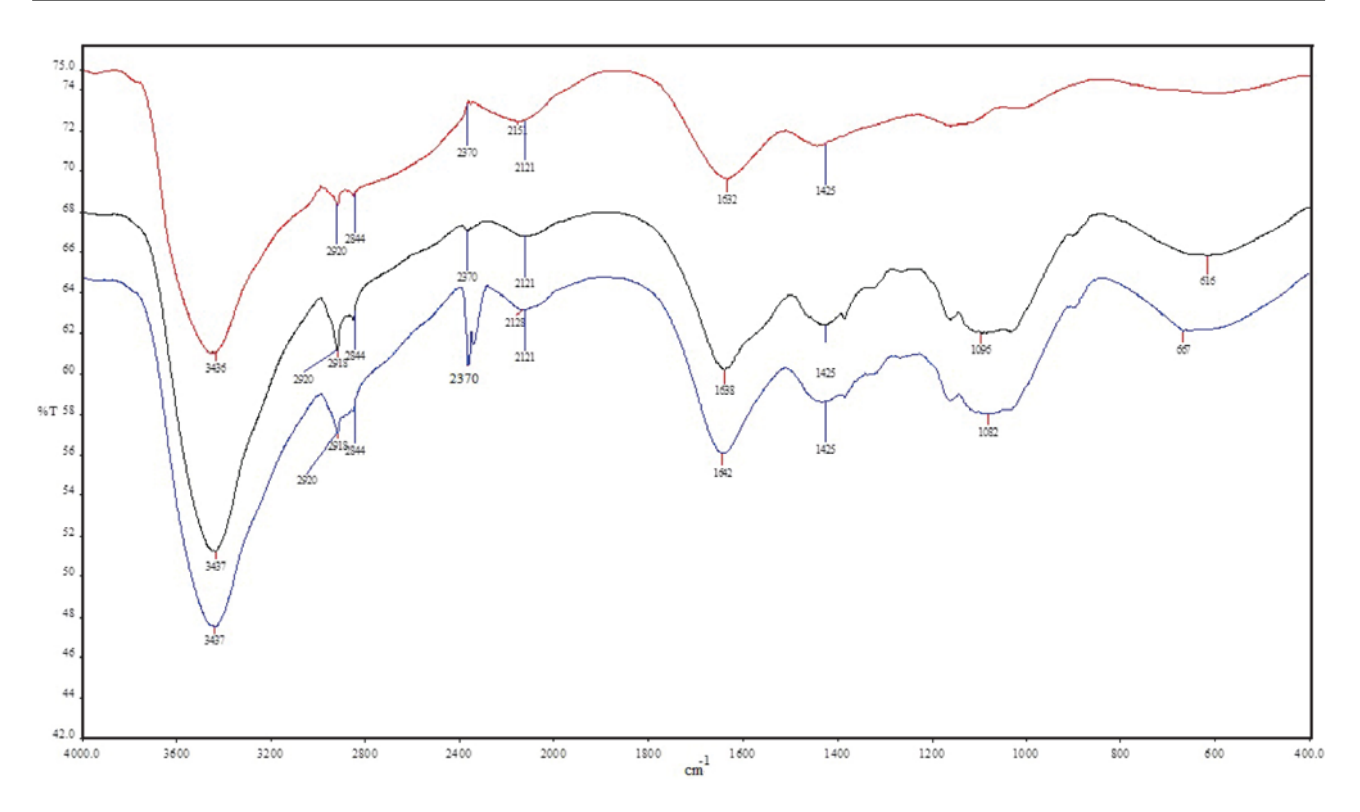


Figure 1. FTIR spectrum of native chitosan film (red) and corn cob film before adsorption (black) and after adsorption (blue)

evenly disperse onto the chitosan matrix. This can be observed from the homogeneity shown by the film (Figure 2a). The energy dispersive X-ray (EDX) analysis was performed on the white spots shown in Figure 2a. The Ti peaks in the spectrum (Figure 3) confirm the presence of TiO_2 in the film. As for corn cob film, it is clear that it is a non-porous type of materials (Figure 4a). Significant dif-

ference was observed on film morphology after it undergoes dye removal process. Both of the film's surfaces displayed less uniformity than before dyes removal. It is suggested that the rough and uneven surfaces shown in these films is due to the adhesion of dye molecules.

Besides SEM, color mapping using contact mode, atomic force microscope (AFM) was also employed to

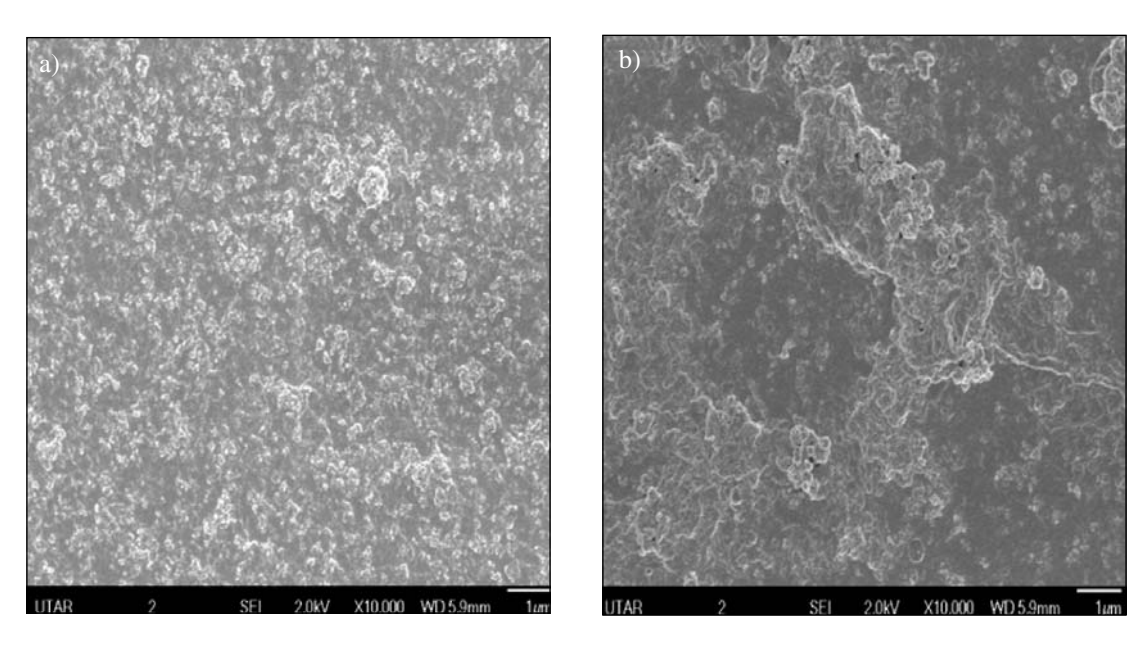


Figure 2. SEM micrographs of ${\rm TiO_2}$ film before (a) and after (b) dyes removal process

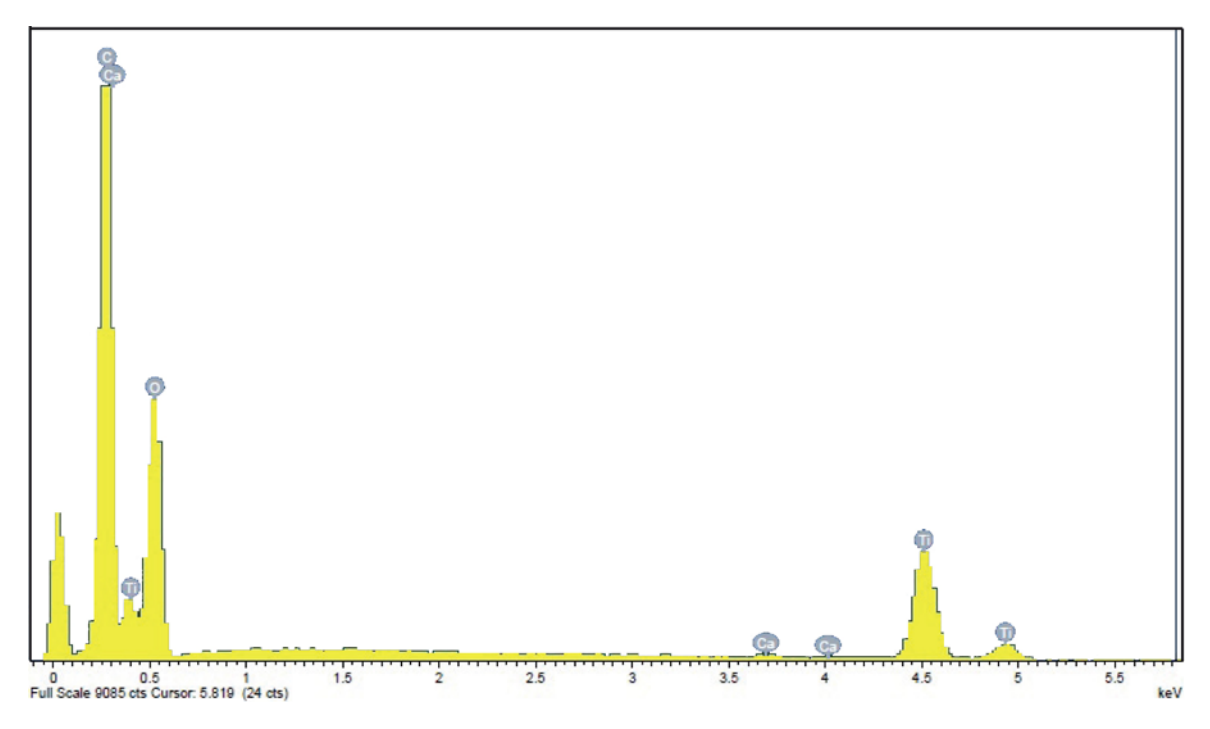


Figure 3. EDX analysis spectrum of the white spot in TiO, film

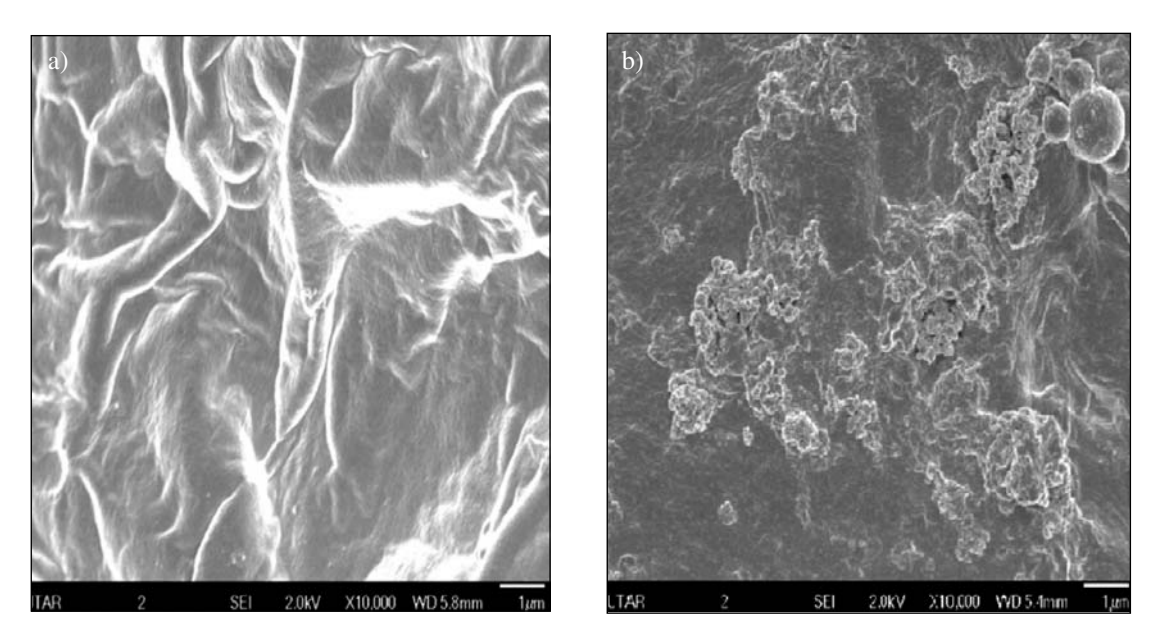


Figure 4. SEM micrographs of corn cob film before (a) and after (b) dyes removal process

define the saturation of film's surface. This is one of the usual methods used for displaying data whereby high features or high topography is illustrated by lighter color and vice versa. From the images obtained (Figures 5–6), films after the dyes removal process exhibited lighter color and rougher surface. This is most probably caused by the agglomeration of dyes. During the removal process, with the introduction of dye molecules on the surface of the films, these films become more intense and this ex-

plains the higher topography shown after the removal process.

3. 2. Effect of Initial pH of Dye Solution

Figure 7 shows the percentage uptake of MG and AY 17 from natural pH of binary dye solution (4.54) to 7 after 4 hours of contact time. The pH of dye solution is a crucial controlling parameter as it is going to influence the

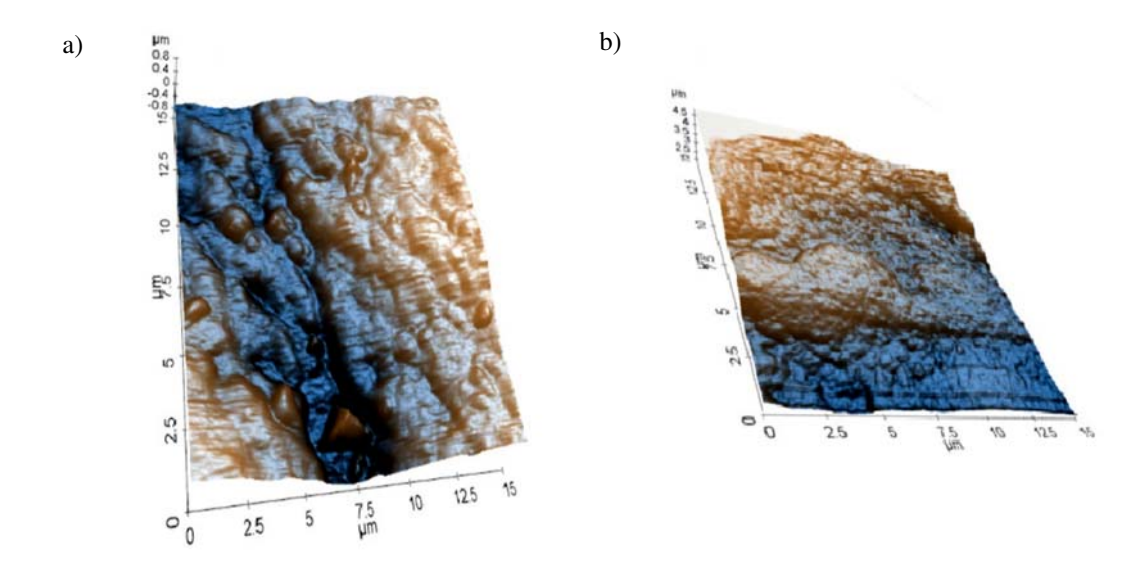


Figure 5. AFM image of TiO₂ film before (a) and after (b) dyes removal process

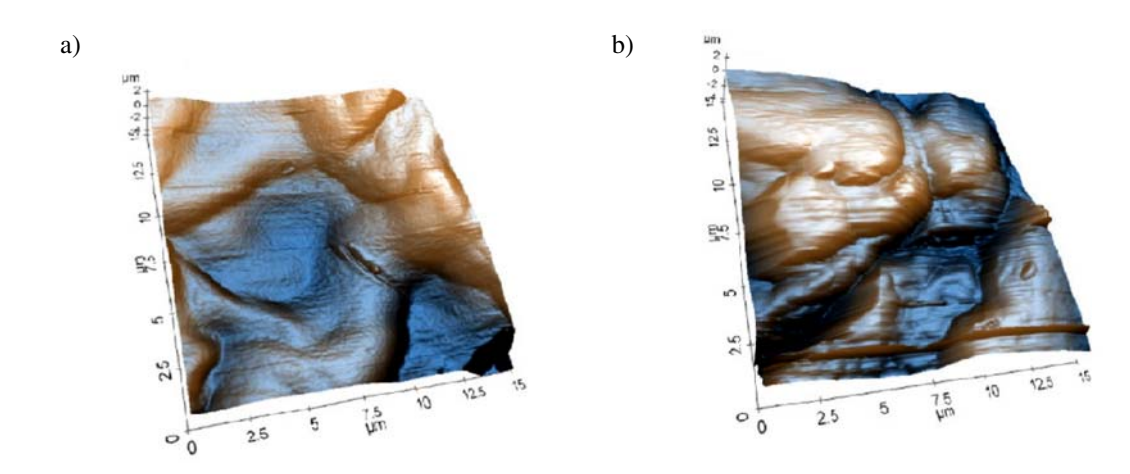


Figure 6. AFM image of corn cob film before (a) and after (b) dyes removal process

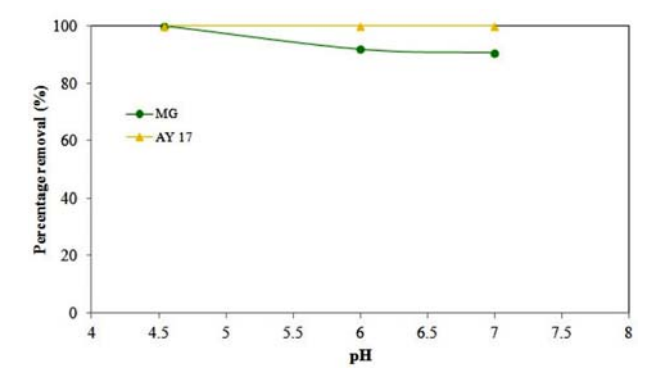


Figure 7. Effect of pH in the removal of MG and AY 17

aqueous chemistry as well as the surface binding sites of adsorbent. ¹⁸ Generally, the removal of MG should be increased as the pH of the solution increased whereas for

AY 17, higher removal will be facilitated at low pH. However, the current results obtained indicated that the removal of both dyes was more favorable in acidic condition and this agreed well with some of the previously reported works. ^{19–21}

The high affinity shown by the films in acidic pH can be attributed to the usage of chitosan as the supporting matrix in this study. At lower pH, amino groups of chitosan can be easily protonated to form –NH₃⁺. With decreasing pH, there will be more protons available to protonate amino groups of chitosan and this enhance the attraction of negatively charged dye (AY 17) towards the cationic amines.^{22,23} However, as chitosan is a type of pH sensitive cellulose biopolymer which will dissolve and formed hydrogel under extreme acidic condition, therefore the effect of pH was not carried out beyond pH 4. And since by using the natural pH of the binary dye solution, an appreciate amount of both dyes could be removed simultane-

ously, therefore no pH adjustment was carried out in subsequent experiments.

3. 3. Effect of Initial Dye Concentration and Contact Time

The influence of the contact time was studied in order to identify the equilibrium time for maximum adsorption. Figure 8 indicates the rates of adsorption of MG and AY 17 at various concentrations. The uptake for three different concentrations which were 20, 40 and 80 mg/L for both MG and AY 17 showed the similar adsorption trend. From the results, it can be noticed that the adsorption of dyes was rapid at beginning, followed by a gradual process. This fast uptake at the beginning may be attributed to the large amount of available vacant binding sites of sorbent whereas a subsequent slower adsorption could be related to intraparticle diffusion. The current uptake pattern followed essentially the same trend in most of the reported works dealing with the adsorption studies whereby it can be customarily classified into rapid formation of an equilibrium interfacial concentration, followed by slow diffusion into the adsorbent.²⁴ With increasing contact time, the percentage uptake of dye removal rate decreased due to limited vacant adsorption sites as the binding sites of sorbent become saturated with dye molecules.²³ Hence, this has turned into a limiting factor for dye uptake. Similar observations were reported in the removal of colored textile wastewater using chitosan and the authors explai-

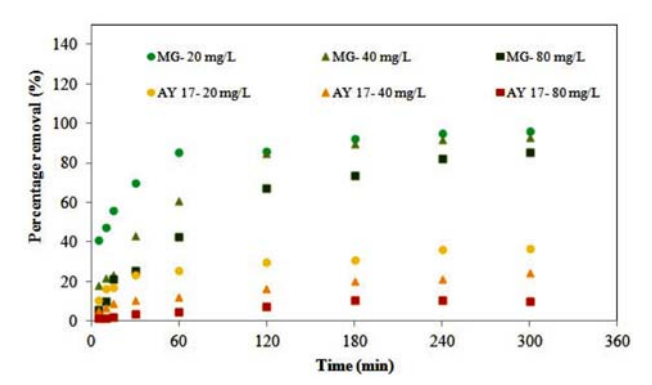


Figure 8. Effect of initial dye concentration and contact time in the removal of MG and AY 17

ned that these were due to the competition for active adsorption sites. ^{20,25} At higher dye concentration, the number of available adsorption sites becomes fewer and many dye molecules competed strongly to the limited adsorption sites. Consequently, large number of dye molecules was not being adsorbed successfully onto the sorbent.

3. 4. Kinetics Studies

Sorption kinetic studies were explored as it can provide some important insight about the mechanism of adsorption processes as well as describe the reaction pathways. The modeling of the kinetic studies of MG and AY 17 onto the sorbent was examined individually by applying two different kinetic models, namely pseudo-first-order²⁶ and pseudo-second-order.²⁷ The applicability of the model was chosen based on their respective linear regression correlation coefficient, R² values.

3. 4. 1. Pseudo-first Order Kinetic Model

For pseudo-first order kinetic model, it assumes that the rate of the solute change is directly proportional to the amount of solid uptake with time. The linear equation of pseudo-first order equation is expressed as follows:

$$\log (q_e - q_t) = \log q_e - \frac{K_t}{2.303} t$$
 (2)

where

 q_e = amount of dyes adsorbed at equilibrium, mg/g

 q_t = amount of dyes adsorbed at time t, mg/g

 K_1 = rate constant of pseudo-first order, 1/min

t = time, min

A linear graph of log $(q_e - q_t)$ versus time for the adsorption of MG and AY 17 onto the corn cob films at the concentration of 20, 40 and 80 mg/L was plotted (Figure not shown). The experimental, $q_{\rm e(expt)}$ and theoretical, $q_{\rm e(cal)}$ adsorption capacities of dye at equilibrium and the first-order rate constant, K_1 with the correlation coefficient, R^2 for each dye concentration of was tabulated in Table 1. The $q_{\rm e(expt)}$ and K_1 were determined from the intercept and gradient of the kinetic plot, respectively. Based on the re-

Table 1. Adsorption capacities, kinetic model parameters and correlation coefficients based on pseudo-first and pseudo-second order kinetic models

Dye	Initial dye	q _{e (expt)}	Pseudo-first order kinetic model			Pseud	Pseudo-second order kinetic model			
	concentration	(mg/L)	${f q_{e\;(cal)}} \ ({f mg/g})$	K ₁ (1/min)	R ² mg/g)	$\begin{matrix}q_{e,\;cal}\\(mg\;g^{-1})\end{matrix}$	K ₂ (1/min)	h (mg/g.min)	\mathbb{R}^2	
MG	20	5.4106	1.4983	0.00253	0.2583	5.0556	0.0286	0.7301	0.9837	
	40	9.8819	5.4425	0.01474	0.5810	11.0375	0.0031	0.3831	0.9960	
	80	14.8624	10.6856	0.01036	0.8083	18.6220	0.0009	0.2971	0.9830	
AY 17	20	2.2865	1.7939	0.006909	0.5023	3.0544	0.0040	0.0370	0.9926	
	40	3.3817	2.1857	0.005297	0.6686	3.5727	0.0074	0.0947	0.9758	
	80	3.2961	1.6749	0.005758	0.4756	3.3852	0.0137	0.1570	0.9887	

sults, for both MG and AY 17, the R^2 values were relatively low and the $q_{e(cal)}$ values gave unreasonable values compared to those determined experimentally. Besides, it was found that the pseudo-first order kinetic equation does not fit well for the whole range of the adsorption process. This clearly indicates the non-applicability of pseudo-first order kinetic model for the studied dyes and implies more than one parameter could be involved in the adsorption process. From the literature, the reviews of experimental works also reveal that (in most cases) the pseudo-first order equation is unable to correlate the measured kinetics well. $^{28-30}$

3. 4. 2. Pseudo-second Order Kinetic Model

The adsorption kinetic data was further studied by using pseudo-second order model. Pseudo-second order model assume that rate limiting step may be chemisorption involving the valence forces transferring through electron sharing or exchanging between sorbent and sorbate as covalent forces, and ion exchange.^{29,31} The linear equation of the model was shown:

$$\frac{t}{q_t} = \frac{1}{h} + \frac{1}{q_s} \tag{3}$$

where $h = K_2 q_e^2$

h = initial rate of adsorption, mg/g.min

 K_2 = rate constant of pseudo-second order, g/mg.min

This model is considered more appropriate to represent the kinetic data in biosorption systems and has the following advantages: it does not have the problem of assigning an effective adsorption capacity, the rate constant of pseudo-second-order, and the initial adsorption rate all can be determined from the equation without knowing any parameter beforehand.²⁹ A linear plot of t/q, versus t for MG and AY 17 at various concentrations was plotted (Figure 9). The h values were calculated from y-intercept, whereas $q_{e \text{ (cal)}}$ and K_2 values were obtained from the gradient of the linear plot. The R² values for both MG and AY 17 were found to be higher and closer to unity. Additionally, based on the tabulated data in Table 1, the theoretical $q_{e \, (cal)}$ shown closer values with the experimental equilibrium adsorption capacities. Therefore, it implies that adsorption of MG and AY 17 were better described by pseudo-second order kinetic model. The pseudo-second order rate constant, K2 was found to be decrease with increasing dye concentrations (Table 1). This could be related to lower competition among the dyes molecules at lower concentration for the limited available surface adsorption sites.²³

The values of q_e , K_2 and h against C_o in the corresponding linear plots of the pseudo-second order kinetic model were regressed in order to obtain the expression for theoretical MG and AY 17 concentration. These parame-

ters could be expressed as a function of C_{o} for MG and AY 17 as follows:

$$q_e = \frac{c_o}{A_a c_o + B_a} \tag{4}$$

$$K_2 = \frac{c_o}{A_b c_o + B_b} \tag{5}$$

$$h = \frac{C_o}{A_h C_o + B_h} \tag{6}$$

where A_q , B_q , A_k , B_k , A_h and B_h are constant for the respective equations and obtained through regression from the linear plots. The generalized predictive models for MG and AY 17 adsorbed at any contact time and initial dye concentrations within the given range with relationship of q_t , C_o and t can be expressed as follow:

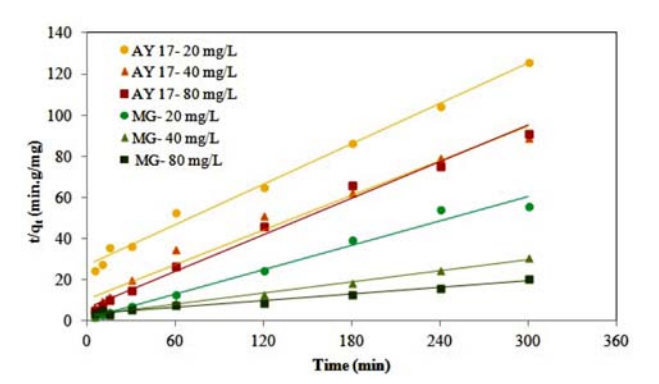


Figure 9. Pseudo second-order kinetics of MG and AY 17

$$q_{t} = \frac{C_{o}t}{(A_{h})(C_{o}) + B_{h} + (A_{q}C_{0} + B_{q})t}$$
(7)

By substituting the calculated constant values, the theoretical model for MG and AY 17 could be represented as equation below:

$$(MG)q_t = \frac{C_o t}{(4.2273)(C_o) - 48.686 + (-0.0184C_0 + 3.6252)t}$$
(8)

$$(AY 17)q_t = \frac{C_o t}{(35.714)(C_o) - 847.28 + (0.3298C_0 - 1.1656)t}$$
(9)

Theoretical model derived for MG and AY 17 was applied to obtain the adsorption capacity, \mathbf{q}_{t} at any given \mathbf{C}_{o} and t. A comparison between the experimental values and theoretical values was shown in Figure 10.

It is clear that the theoretically generated curves showed good agreement with experimental data for 20 mg/L of MG, but deviations occurred at higher concentrations. This deviation could be related with the formation of multilayers on the sorbent as the dye concentrations in-

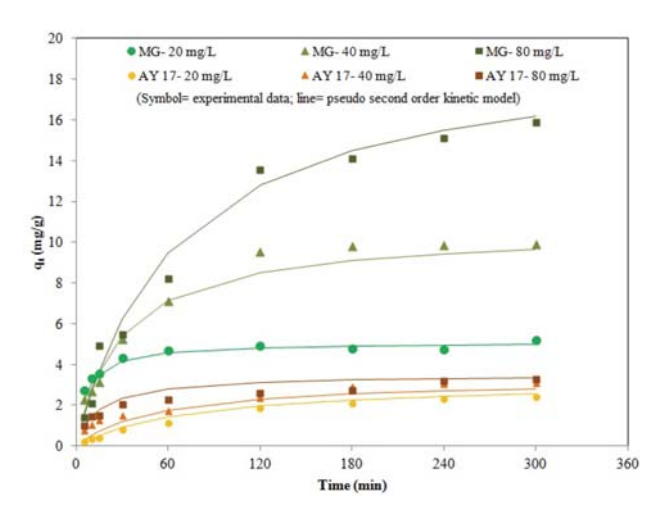


Figure 10. Typical plots of comparison between the measured and pseudo second order modeled time profiles for MG and AY 17 removal

creased. ³² Additionally, deviations were more pronounced in the case of AY 17 and this might be due to the poor R^2 values of the linear graph of q_e , K_2 and h against C_o . Several studies have also reported the suitability of pseudo-second order kinetic model in describing the adsorption process. ^{33–35}

3. 5. Sorption Isotherm

The sorption isotherm is important as it can be used to describe the interaction between sorbent surface and the dyes molecules. Two different isotherm models were applied, namely Langmuir ³⁶ and Freundlich³⁷ models which are capable to give some insight into the sorption mechanism and the distribution between sorbate molecules and affinities of the sorbent. The most appropriate correlation equilibrium model was determined based on their respective isotherm constant and correlation coefficient, R² value.

The equation of Langmuir isotherm was shown below:

$$\frac{C_e}{q_e} = \frac{C_e}{q_m} + \frac{1}{K_a q_m} \tag{10}$$

where,

C_e = Equilibrium liquid phase dye concentration (mg/L) q_e = Amount of dye absorbed at equilibrium (mg/g) q_{...} = Maximum adsorption capacity (mg/g)

 $K_a = Adsorption equilibrium constant (L/mg)$

A linear graph of C_e/q_e against C_e for the adsorption of MG and AY 17 onto corn cob films was plotted and shown in Figures 11 and 12, respectively. The correlation

shown in Figures 11 and 12, respectively. The correlation coefficient, R² value was 0.9406 for the linear plot of MG, whereas R² for AY 17 was 0.9684. This result indicates that monolayer adsorption of AY 17 on the surface of corn

cob films system fitted better in Langmuir isotherm, but not for MG. The plot gave a linear regression line provided with gradient of $1/q_{\rm m}$ and y-intercept of $1/q_{\rm m}K_{\rm a}$. The maximum adsorption capacity, $q_{\rm m}$ for MG and AY 17 were calculated as 35.336 mg/g and 0.241 mg/g, respectively. Meanwhile, Langmuir isotherm constant for the adsorption of MG was 0.882 L/mg and AY 17 was 0.039 L/mg.

In Langmuir isotherm, another important characteristic is that be related to the dimensionless equilibrium parameter, $R_L^{\ 38}$ and the values could be calculated by using the equation shown as follow:

$$R_L = \frac{1}{1 + K_a C_o} \tag{11}$$

where,

 $R_L = Dimensionless equilibrium parameter$

 $K_a = Adsorption equilibrium constant (L/mg)$

 $C_0 =$ Initial concentration of dye solution (mg/L)

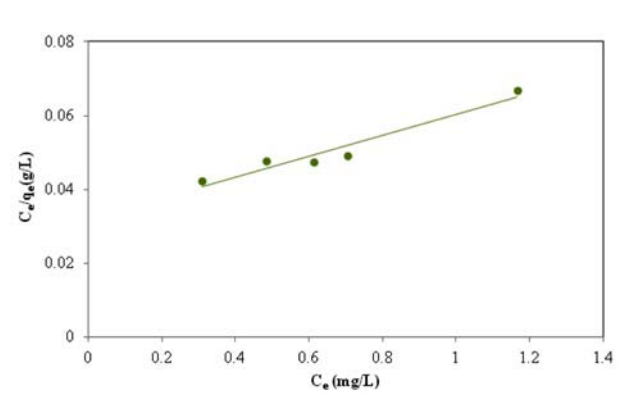


Figure 11. Langmuir isotherm of MG

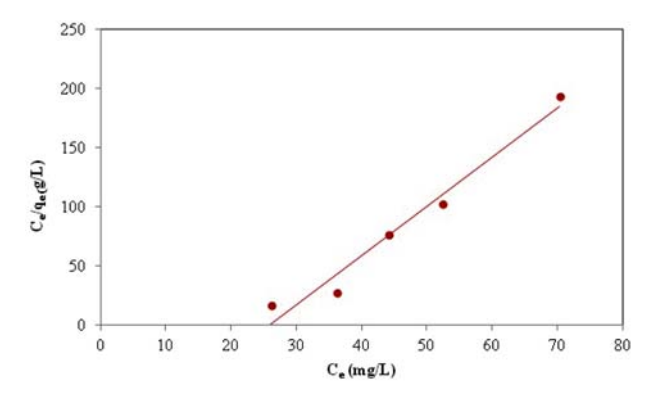


Figure 12. Langmuir isotherm of AY 17

The favorability of MG and AY 17 adsorption system could be predicted based on R_L value (If $R_L > 1$, unfavorable; $R_L =$, linear; $0 < R_L < 1$, favorable; $R_L = 0$, irreversible). The calculated R_L value lies between 0.0207 to 0.4534 and this indicates that the adsorption process

is favorable and corn cob thin films is a potential adsorbent for the removal of MG and AY 17 from aqueous solution.

The Freundlich isotherm assumes a physiochemical multilayer adsorption process on heterogeneous surfaces energy system. This isotherm is more towards a non-ideal adsorption that is more flexible and does not assume adsorption limit. The exponential Freundlich isotherm model equation is expressed as:

$$q_e = K_F C_e^{1/n} \tag{12}$$

where K_F = Freundlich isotherm constant for adsorption and n = Freundlich constant for intensity of adsorption. By taking the logarithm, the equation will therefore be in a linearized form and appeared as below:

$$\log q_s = \log K_F + \frac{1}{n} \log C_s \tag{13}$$

The graphs of log q_e against log C_e for MG and AY 17 were plotted and shown in Figures 13 and 14, respectively. The linear regression line on the plot could be used to determine the value of 1/n and K_F from gradient and y-intercept, respectively. The coefficients for the linearized forms of the isotherm models for the adsorption of both dyes are listed in Table 2. The results implied that adsorption of MG on the corn cob films was more towards the heterogeneous surface and belong to multilayer adsorption system. The values of n for MG and AY 17 were 1.484 and -0.618 whereas the intensities of Freundlich

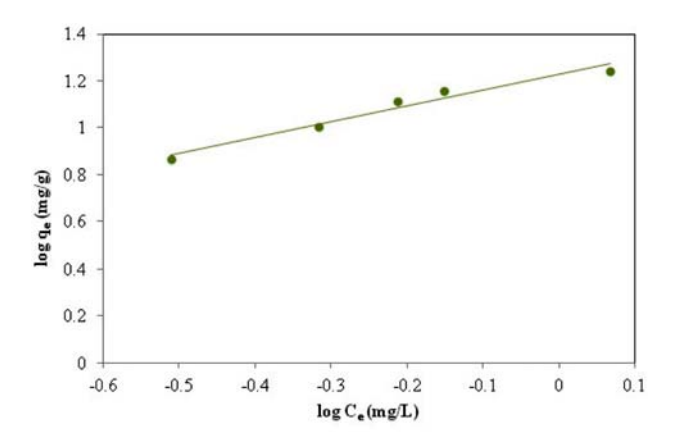


Figure 13. Freundlich isotherm of MG

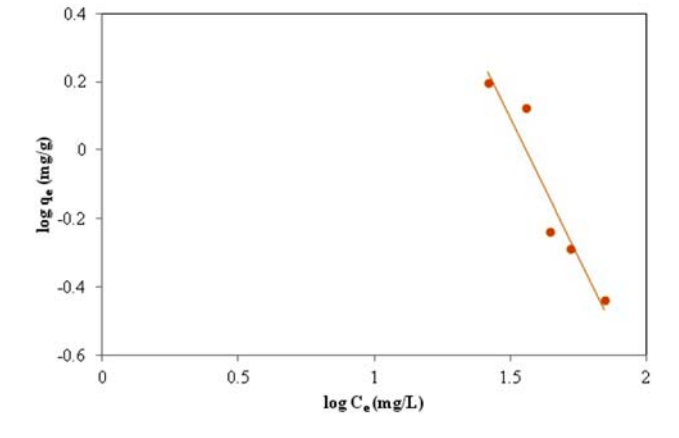


Figure 14. Freundlich isotherm of AY 17

constant were 16.881 and 333.657, respectively. Adsorption system will be termed as favorable process when the n value is in the range of 1 < n < 10. Based on the n value obtained, the adsorption of MG was termed as favorable. As for AY 17, Langmuir model appears to provide a more reasonable fitting and therefore this explains why a lower n value was obtained.

3. 6. Reusability of TiO₂ Film and Corn Cob Film

Reusability is a major concern as this is one of key steps to make this type of economical dyes removal method applicable for practical usage. Therefore, a study on the repetitive usage and recycle of the thin films was performed. Figure 15 shows the effect of repetitive usage of TiO₂ and corn cob films on the percentage removal of MG and AY 17. The percentage removal of MG was maintained around 90 % whereas percentage removal of AY 17 decreased from cycle 1 to 4. This can be attributed by the non-negligible adsorbed dye molecules on the films. Although the film was subjected to regeneration process by using NaOH before the next cycle of usage, some of the AY 17 dye molecules might still be strongly bind to the films and this condition hinders other AY 17 dye molecules from reaching to the active site and subsequently, a lower uptake was observed. As for MG, the recycling method adopted shown that this is a suitable method to desorb the previously attached MG dye and as a result, a high removal efficiency was maintained throughout the process.

Table 2. Langmuir and Freundlich isotherm parameters

D		Langmuir	Freundlich			
Dye	q_m , mg/g	K _a , L/mg	\mathbb{R}^2	$\mathbf{K}_{\mathbf{F}}$	n	\mathbb{R}^2
MG	35.336	0.882	0.9406	16.881	1.484	0.9633
AY 17	0.241	0.039	0.9684	333.657	-0.618	0.9081

3. 7. Statistical Experimental Design-Plackett-Burman (PB) and Response Surface Methodology (RSM)

Statistical approach was employed to determine the important factors and to optimize the experimental condition for the removal of MG and AY 17 in binary dye solution. Design-Expert version 7.1.3 was used to validate the model through function of desirability. Significant factors that affect the dyes removal through combination of photodegradation and adsorption were screened through Plackett- Burman (PB) design.

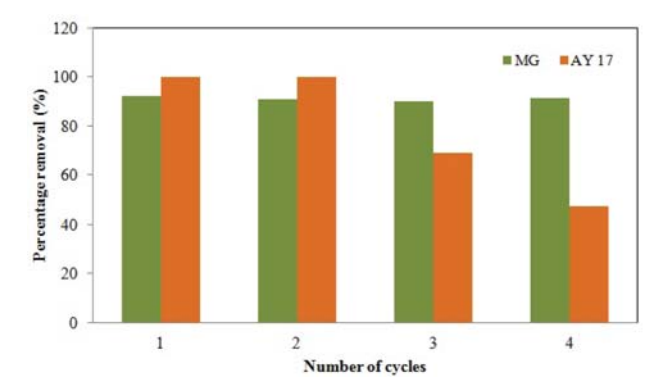


Figure 15. Effect of reusability in the removal of MG and AY 17

A total of three assigned parameters which were initial dye concentrations, contact time and pH were screened in total 12 experimental runs. For both MG and AY 17, the generated experimental condition and the differences of % removal between observed and predicted values were calculated and shown in Tables 3 and 4, respectively. It was observed that the largest and smallest differences between the observed and predicted removal for MG were 1.97% and 13.57%, respectively. As for AY 17, the percentage of differences was recorded in the range of 0.21% to 18.61%. The differences shown between the experimental and predicted percentage of removal is

most probably due to the involvement of insignificant variables in the analysis. In some of the previously reported works, the researchers also noticed that there'll some differences in terms of the observed and predicted response and they attributed this kind of deviation to the non-negligible effect of insignificant variables in the design.^{2,32}

Table 5 shows the analysis of variance (ANOVA) of both MG and AY 17 in binary dye solution. The studied variables were identified as significant Prob > F was less than 0.05. Based on the value, the studied model was found to be significant. For both MG and AY 17, the significant factors in affecting the removal process were contact time and initial pH of binary dye solution. The effect of contact time was termed as significant and this is closely related to the involvement of various stages in the process of adsorption. As for the effect of pH, this suggests that the degree of ionization of the adsorbate and the surface properties of the adsorbent play an important role in determining the efficiency of the process.

The influential factors identified through PB were further studied and optimized using response surface methodology (RSM). A total of 13 experimental runs were conducted and Table 6 shows the combination of the generated contact time and initial pH. Besides, the observed and predicted response was also presented in the same table. The modified cubic model was employed to describe the correlation between these two important factors and the percentage removal was shown as follows in terms of coded form:

MG in binary dye solution:

% uptake of MG =
$$+94.16 + 16.95 \text{ A} - 10.04 \text{ B} - 9.18 \text{ AB} - 15.96 \text{ A}^2 - 11.36 \text{ B}^2$$
 (14)

AY 17 in binary dye solution:

% uptake of AY 17 =
$$+101.87 + 35.05 \text{ A}$$

- $10.06B - 12.41 \text{ AB} - 50.89 \text{ A}^2 - 6.53 \text{ B}^2$ (15)

Where A = contact time and B = initial pH

Table 3. Plackett-Burman design and results for the percentage removal of MG in binary dye solution

Experiment	Contact time,	Variable Initial concentration, mg/L	pН	Observed response, %	Predicted response, %	Differences,
1	240.00	10.00	7.00	54.05	59.51	-5.46
2	240.00	10.00	7.00	54.05	59.51	-5.46
3	240.00	10.00	4.54	96.74	83.17	13.57
4	240.00	20.00	4.54	93.22	88.43	4.79
5	5.00	20.00	7.00	42.54	44.52	1.97
6	240.00	20.00	7.00	52.54	64.77	-12.23
7	5.00	20.00	4.54	47.08	58.94	-11.86
8	5.00	20.00	7.00	42.54	44.52	1.97
9	5.00	10.00	7.00	38.68	44.52	1.97
10	5.00	10.00	4.54	48.04	53.69	-5.65
11	5.00	10.00	4.54	48.04	53.69	-5.65
12	240.00	20.00	4.54	93.22	88.43	4.79

Tables 7 and 8 were the ANOVA results and from these tables, both models were found to be significant (P < 0.0001) with model F-value of 102.21 and 36.37 for MG

and AY 17, respectively. The relatively high R² values in MG and AY 17 models indicated that there were good agreements between the experimental and predicted va-

Table 4. Plackett-Burman design and results for the percentage removal of AY17 in binary dye solution

Experiment	Contact time,	Variable Initial concentration, mg/L	pН	Observed response, %	Predicted response, %	Differences,
1	5.00	40.00	4.54	11.90	20.60	-8.70
2	5.00	40.00	4.54	11.90	20.60	-8.70
3	240.00	60.00	4.54	100.00	91.89	8.11
4	240.00	40.00	7.00	47.26	53.98	-6.72
5	5.00	60.00	4.54	13.68	28.33	-14.65
6	240.00	60.00	7.00	43.10	61.71	-18.61
7	240.00	60.00	4.54	100.00	91.89	8.11
8	240.00	40.00	7.00	47.28	53.98	-6.70
9	5.00	60.00	7.00	6.67	7.31	-0.64
10	5.00	60.00	7.00	6.67	7.31	-0.64
11	5.00	40.00	7.00	5.43	5.22	0.21
12	240.00	40.00	4.54	100.00	84.16	15.84

Table 5. Regression analysis (ANOVA) of Placktt-Burman of MG and AY 17 in binary dye solution

Dye	Source	Degree of freedom	Sum of squares	Mean square	F-value	Prob > F	Description
MG	Model	3	4369.61	1456.54	14.14	0.0015	Significant
	Contact time	1	2607.80	2607.80	25.32	0.0010	Significant
	Initial MG concentration	1	82.90	82.90	0.80	0.3958	Not significant
	Initial pH	1	1678.91	1678.91	16.30	0.0037	Significant
	Residual	8	823.92	102.99	_	_	_
AY 17	Model	3	15032.24	5010.75	25.77	0.0002	Significant
	Contact time	1	12120.26	12120.26	62.33	0.0001	Significant
	Initial AY 17 concentration	1	179.18	179.18	0.92	0.3652	Not significant
	Initial pH	1	2732.80	2732.80	14.05	0.0056	Significant
	Residual	8	1555.58	194.45	-	_	_
	Total	11	16587.82		_	_	_

Table 6. Central composite design (CCD) matrix for two independent variables and the observed respond on MG and AY 17 in binary dye solution

	variat	ole						
Experiment	Contact time	Initial pH	Experimental % uptake of MG	Predicted % uptake of MG	Differences, %	Experimental % uptake of AY 17	Predicted % uptake of AY 17	Differences,
1	122.50	5.77	93.1	93.28	-0.18	100	100	0.00
2	240.00	7.00	62.75	64.58	-1.83	45.02	57.03	-12.01
3	122.50	4.54	96.7	93.28	3.42	100	100	0.00
4	5.00	7.00	49.39	49.03	0.36	9.05	11.75	-2.70
5	122.50	5.77	93.1	93.28	-0.18	100	100	0.00
6	122.50	5.77	93.1	93.28	-0.18	100	100	0.00
7	240.00	5.77	100	95.16	4.84	100	86.03	13.97
8	122.50	5.77	93.1	93.28	-0.18	100	100	0.00
9	122.50	5.77	93.1	93.28	-0.18	100	100	0.00
10	240.00	4.54	100	93.28	6.72	100	100	0.00
11	5.00	4.54	49.93	50.76	-0.83	14.4	7.05	7.35
12	5.00	5.77	61.73	61.26	0.47	11.28	15.93	-4.65
13	122.50	7.00	74.23	72.76	1.47	100	85.28	14.72

Table 7. Regression analysis (ANOVA) of RSM of MG

Source	Degree of freedom	Sum of squares	Mean square	F-value	p-value (Prob>F)	Description
Model	5	4351.68	870.34	102.21	< 0.0001	Significant
A	1	1723.81	1723.81	202.44	< 0.0001	Significant
В	1	605.21	605.21	71.08	< 0.0001	Significant
AB	1	336.91	336.91	39.57	0.0004	Significant
A^2	1	703.36	703.36	82.60	< 0.0001	Significant
$\mathbf{B^2}$	1	356.31	356.31	41.85	0.0003	Significant
Residual	7	59.61	8.52	_	_	_

R²: 0.9865, Adjusted R²: 0.9768, Predicted R²: 0.8937, Adequate precision: 27.233 and C.V.: 3.58 %

Table 8. Regression analysis (ANOVA) of RSM of AY 17

Source	Degree of freedom	Sum of squares	Mean square	F-value	p-value (Prob>F)	Description
Model	5	17914.53	3582.91	36.37	< 0.0001	Significant
\mathbf{A}	1	7370.31	7370.31	74.82	< 0.0001	Significant
В	1	606.62	606.62	6.16	0.0421	Significant
AB	1	615.78	615.78	6.25	0.0410	Significant
$\mathbf{A^2}$	1	7152.23	7152.23	72.61	< 0.0001	Significant
\mathbf{B}^2	1	117.70	117.70	1.19	0.3105	Not significant
Residual	7	689.54	98.51	-	_	-

R²: 0.9629, Adjusted R²: 0.9365, Predicted R²: 0.6454, Adequate precision: 14.585 and C.V.: 13.17 %

lues. The R² that is close to unity signified a stronger model and it would be able to provide a better response.³⁹ The signal to noise ratio is represented by adequate precision and a ratio that is greater than 4 is desirable.^{40, 41} From this study, the adequate precision for MG and AY 17 models were 27.233 and 14.585, respectively and this shown an adequate signal. The coefficient of variance (C.V.) of MG model was recorded as 3.58% wheraeas for AY 17 model was 13.17%. A low value of C.V. is preferred as this represents a greater precision and reliability of the experiments carried out.⁴⁰ As both models have shown an adequate signal, therefore they were used to navigate the design space.

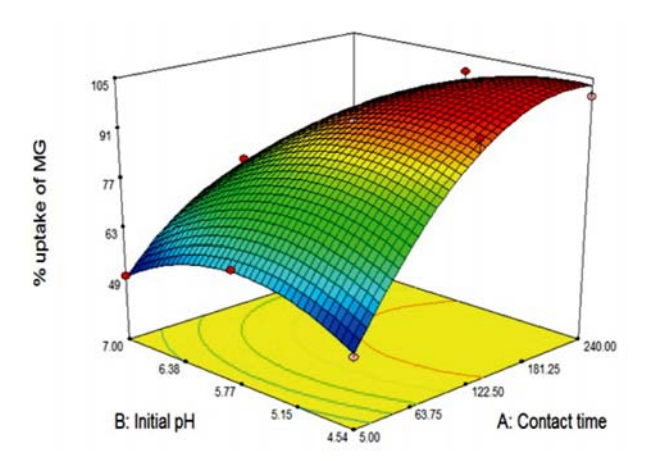


Figure 16. 3D surface plot of MG as a function of initial pH and contact time

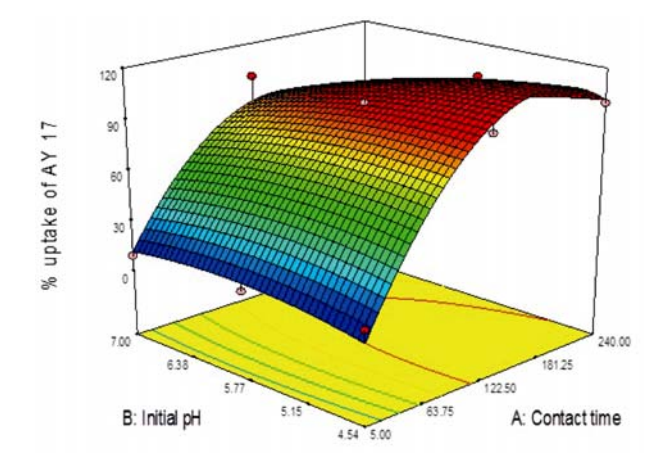


Figure 17. 3D surface plot of AY 17 as a function of initial pH and contact time

Figures 16 and 17 showed the 3D surface plot of MG and AY 17, respectively for the interaction between contact time and initial pH. For the removal of both dyes, a more favourable condition was observed when the contact time was at the maximum point while initial pH was at the minimum point within the studied range. This is because by prolonging the contact time, it leads to more diffusion time and therefore a greater amount of dye molecules can be adsorbed onto the sorbent sites. As for the effect of initial pH, again, this is related to the surface charge and the usage of chitosan as the immobilizing agent.

4. Conclusion

The results from this study have shown the effectiveness of TiO2 and corn cob films in the removal of MG and AY 17 from aqueous solution. The kinetics of dyes adsorption revealed that dye adsorption was more appropriately described by pseudo-second order model which is a kind of chemisorption process, involving valency forces through the sharing or exchange of electrons between the adsorbent and adsorbate as covalent forces, and ion exchange. The equilibrium data obtained was best conformed to Freundlich isotherm for MG and Langmuir isotherm for AY 17. This indicated that the adsorption of both dyes followed their respective heterogeneous and homogeneous adsorption pattern. The maximum adsorption capacity of MG and AY 17 was 35.336 and 0.241 mg/g, respectively. It is interesting to note that the efficiency of the films remained high after being repeated used for 2 cycles. From the statistical experimental design, it was shown that both models were highly significant with relatively high R² values. Within the studied range, the crucial factors in affecting the percentage of removal for both dyes were identified to be contact time and initial pH.

5. Acknowledgements

The authors are thankful for the financial support provided by the Malaysia-Toray Science Foundation through the research grant: 4417/O02. The research facilities provided by Universiti Tunku Abdul Rahman (UTAR) are acknowledged.

6. References

- V. K. Gupta and Suhas, J. Environ. *Manage.*, 2009, 90, 2313–2342.
 - https://doi.org/10.1016/j.jenvman.2008.11.017
- 2. S. L. Lee, S. W. Liew and S. T. Ong, *Acta Chim. Slov.*, **2016**, *63*, 144–153. https://doi.org/10.17344/acsi.2015.2068
- 3. S. Srivastava, R. Sinha and D. Roy, *Aquat. Toxicol.*, **2004**, 66, 319–329.
 - https://doi.org/10.1016/j.aquatox.2003.09.008
- E. Sudova, J. Machova, Z. Svobodova and T. Vesely, Veterinarni Medicina, 2007, 52, 527–539.
- S. T. Ong, S. T. Ong, Y. T. Hung and Y. P. Phung, *Desalin. Water Treat.*, 2015, 55, 1359–1371. https://doi.org/10.1080/19443994.2014.925830
- J. F. Gao, Q. Zhang, K. Su, R. N. Chen and Y. Z. Peng, *J. Hazard. Mater.*, 2010, 174, 215–225. https://doi.org/10.1016/j.jhazmat.2009.09.039
- M. A. Ashraf, M. Hussain, K. Mahmood, A. Wajid, M. Yusof, Y. Alias and I. Yusoff, Desalin. *Water Treat.*, 2013, 51, 4530–4545.
 https://doi.org/10.1080/19443994.2012.747187

- 8. L. Zheng, Z. Dang, X. Yi and H. Zhang, J. Hazard. *Mater.*, **2010**, *176*, 650–656.
 - https://doi.org/10.1016/j.jhazmat.2009.11.081
- 9. A. Buasri, N. Chaiyut, K. Tapang, S. Jaroensin and S. Panphrom, *APCBEE Procedia*, **2012**, *3*, 60 64. https://doi.org/10.1016/j.apcbee.2012.06.046
- B. Barl, C. Biliaderis, E. Murray and A. Macgregor, J. Sci. *Food Agric.*, **1991**, *56*, 195–214. https://doi.org/10.1002/jsfa.2740560209
- L. Suhadolnik, A. Pohar, B. Likozar and M. Čeh, *Chem. Eng. J.*, **2016**, *303*, 292–301. https://doi.org/10.1016/j.cej.2016.06.027
- 12. M. Krivec, A. Pohar, B. Likozar and G. Dražić, *AIChE J.*, **2015**, *61*, 572–581. https://doi.org/10.1002/aic.14648
- M. Bitenc, B. Horvat, B. Likozar, G. Dražić and Z.C. *Orel*, *Appl. Catal.*, B., **2013**, *136*– *137*, 202– 209. https://doi.org/10.1016/j.apcatb.2013.02.016
- F. Han, V. S. R. Kambala, M. Srinivasan, D. Rajarathnam and R. Naidu, *Appl. Catal.*, *A.*, **2009**, *359*, 25–40. https://doi.org/10.1016/j.apcata.2009.02.043
- 15. M. A. Rauf and S. Salman Ashraf, *Chem. Eng.* J., **2009**, *151*, 10–18. https://doi.org/10.1016/j.cej.2009.02.026
- J. M. Herrmann, Catal. Today, 1999, 53, 115–129. https://doi.org/10.1016/S0920-5861(99)00107-8
- K. A. M. Amin and M. Panhuis, *Polymers*, **2012**, *4*, 590–599. https://doi.org/10.3390/polym4010590
- S. L. Chan, Y. P. Tan, A. H. Abdullah and S. T. Ong, J. Taiwan *Inst. Chem. Eng.*, 2016, 61, 306–315. https://doi.org/10.1016/j.jtice.2016.01.010
- M. S. M. Hassan, Radiat. *Phys. Chem.*, **2015**, *115*, 55–61. https://doi.org/10.1016/j.radphyschem.2015.05.038
- N. M. Mahmoodi, R. Salehi, M. Aramin and H. Bahrami, *Desalination*, 2010, 267, 64–72. https://doi.org/10.1016/j.desal.2010.09.007
- 21. Y. P. Phung, S. T. Ong and P. S. Keng, *J. Chem.*, **2013**, *Article ID 3887865*, 1–7. https://doi.org/10.1155/2013/387865
- 22. H. Momenzadeh, B. A. R. Tehrano, A. Khosravi, K. Gharanjig and K. Holmberg, *Desalination*, **2011**, 271, 225–230. https://doi.org/10.1016/j.desal.2010.12.036
- M. Li, S. Wang, W. Luo, H. Xia, Q. Gao and C. Zhou, J. Chem. *Technol. Biotechnol.*, 2014, 90, 1124–1134. https://doi.org/10.1002/jctb.4433
- 24. S. T. Ong, S. T. Ha, P. S. Keng, C. K. Lee and Y. T. Hung. In *Handbook of Environmental and Waste Management*; Yung-Tse Hung, Lawrence K. Wang, Nazih Shammas (Eds); World Scientific Publishing Co.: Singapore, 2012; 929–978. https://doi.org/10.1142/9789814327701_0021
- R. D. C. Soltani, A. R. Khataee, M. Safari and S. W. Joo, Int. Biodeterior. Biodegradation, 2013, 85, 383–391. https://doi.org/10.1016/j.ibiod.2013.09.004
- S. Lagergren and B. K. Svenska, Veternskapsakad Handlingar, 1898, 24, 1–39.
- 27. Y. S. Ho and G. McKay, *Process Biochem.*, **1999**, *34*, 451–465. https://doi.org/10.1016/S0032-9592(98)00112-5
- 28. W. Plazinski, Adv. Colloid *Interface Sci.*, **2013**, *197–198*, 58–67. https://doi.org/10.1016/j.cis.2013.04.002

- Y.S. Ho, J Hazard Mater, 2006, B136, 681–689. https://doi.org/10.1016/j.jhazmat.2005.12.043
- J. Febrianto, A.N. Kosasih, J. Sunarso, Y. H. Ju, N. Indraswati, N. and S. Ismadji, *J Hazard Mater*, **2009**, *162*, 616–645. https://doi.org/10.1016/j.jhazmat.2008.06.042
- 31. Ho, Y. S. and G. McKay, *Water Res.*, **2000**, *34*, 735–742. https://doi.org/10.1016/S0043-1354(99)00232-8
- 32. S. T. Ong and C. K. Seou, Desalin. *Water Treat.*, **2014**, 52, 7673–7684.
 - https://doi.org/10.1080/19443994.2013.830684
- P. Saha, S. Chowdhury, S. Gupta, I. Kumar and R. Kumar, *Clean Soil, Air and Water*, 2000, 38, 437–445. https://doi.org/10.1002/clen.200900234
- 34. T. Santi and S. Manonmani, Malachite Green Removal from aqueous solution by the peel of *Cucumis Sativa* fruit. *Clean Soil, Air and Water*, **2011**, *39*, 162–170. https://doi.org/10.1002/clen.201000077

- K. T. Karthikeyan and Jothivenkatachalam, J. Environ. *Nanotechnol.*, **2014**, *3*, 69–80.
 https://doi.org/10.13074/jent.2014.03.142070
- I. Langmuir, J. Am. Chem. Soc., 1918, 40, 1361–1403. https://doi.org/10.1021/ja02242a004
- 37. H. Freundlich, Phys. Chem. Soc., 1906, 40, 1361-1368
- T. W. Weber and R. K. Chakkravorti, Am. Ins. Chem. Eng. J., 1974, 20, 228–238. https://doi.org/10.1002/aic.690200204
- 39. K. Chauhan, U. Trivedi, and K. C. Patel, *J. Microbial Biotechnol.*, **2006**, *16*, 1410–1415.
- J. K. Kim, B. R. Oh, H. Shin, C. Eom and S. W. Kim, *Process Biochem.*, 2008, 43, 1308–1312. https://doi.org/10.1016/j.procbio.2008.07.007
- 41. E. C. Khoo, S. T. Ong, Y. T. Hung and S. T. Ha, Desalin. *Water Treat.*, **2013**, *51*, 7109–7119. https://doi.org/10.1080/19443994.2013.791774

Povzetek

Proučevana je bila učinkovitost uporabe filmov z vsebnostjo TiO₂ oziroma mikrodelcev koruznih storžev za odstranjevanje barvil malahitno-zeleno (MG) in kislo-rumeno 17 (AY 17) iz raztopine. Uporabljena metoda imobilizacije se lahko izogne filtraciji, ki v praksi ni primerna. V šaržnih eksperimentih so bili pročevani začetni pH raztopine, začetna koncentracija barvila, kontaktni čas in ponovna uporaba adsorbenta. Ravnotežni podatki za MG in AY 17 sledijo Freundlichovi in Langmuirjevi izotermi. Odstotek odstranjenega MG je ostal visok po štirih sorpcijskih ciklih, vendar je bila za AY 17 dosežena višja redukcija. Odstranjevanje obeh barvil je bilo modelirano in optimirano s pomočjo metode po Plackett-Burmanu (PB) in metode odzivne površine (RSM). Pogoji na površini so bili analizirani s pomočjo infrardeče spektroskopije (IR), fourierjeve transformacijske infrardeče spektroskopije (FTIR), elektronske vrstične mikroskopije (SEM) in mikroskopije na atomsko silo (AFM).